Title

Oncogenic drivers dictate immune control of acute myeloid leukemia.

Authors

Rebecca J. Austin[1,2,*], Jasmin Straube[1,2*], Rohit Halder[1], Yashaswini Janardhanan[1], Claudia Bruedigam[1,2], Matthew Witkowski[3,4], Leanne Cooper[1], Amy Porter[1], Matthias Braun[1], Fernando Souza-Fonseca-Guimaraes[5], Simone A Minnie[1,6], Emily Cooper[1], Sebastien Jacquelin[1,6], Axia Song[1], Tobias Bald[1,7], Kyohei Nakamura[1], Geoffrey R. Hill[1,8], Iannis Aifantis[3], Steven W. Lane[1,2,9ϕ], Megan J. Bywater[1,2ϕ].

*, ϕ These authors contributed equally to the manuscript.

Affiliations

[1] Cancer Program, QIMR Berghofer Medical Research Institute, Brisbane, Australia, 4006.

[2] The University of Queensland, St Lucia, Brisbane, QLD, Australia, 4072.

[3] Department of Pathology, NYU School of Medicine, New York, NY 10016, USA; Laura & Isaac Perlmutter Cancer Center, NYU School of Medicine, New York, NY 10016, USA.

[4] Department of Pediatrics, University of Colorado Anschutz Medical Campus, Aurora, Colorado 80045, USA

[5] Frazer Institute, The University of Queensland, Woolloongabba, QLD 4102, Australia

[6] Mater Research, Translational Research Institute, The University of Queensland, Woolloongabba, QLD 4102, Australia

[7] Institute of Experimental Oncology, University Hospital of Bonn, 53127 Bonn, Germany.

[8] Translational Science and Therapeutics Division, Fred Hutchinson Cancer Centre, Seattle Cancer Care Alliance. Seattle, WA.

[9] Cancer Care Services, Royal Brisbane and Women's Hospital, Herston, Australia, 4029.

Running title (60 characters):

Oncogene specific immune responses in AML

Keywords (5):

Acute myeloid leukemia

Immunoediting

Cancer

Oncogene

Immunotherapy

Additional information:

Financial support. SWL is the recipient of the CSL Centenary Fellowship and NHMRC Investigator Grant, which funded this work.

Corresponding author info:

Dr. Steven Lane: steven.lane@qimrberghofer.edu.au

Dr. Megan Bywater: megan.bywater@qimrberghofer.edu.au

SWL has participated in advisory boards for Celgene, Novartis and Janssen, and has received research funding from Janssen and Celgene/ Bristol Myers Squibb for unrelated projects.

GRH has consulted for Generon Corporation, NapaJen Pharma, iTeos Therapeutics, Neoleukin Therapeutics and has received research funding from Compass Therapeutics, Syndax Pharmaceuticals, Applied Molecular Transport, Serplus Technology, Heat Biologics, Laevoroc Oncology, Genentech and iTeos Therapeutics.

FSFG is a consultant and has a funded research agreement with Biotheus Inc.

Word count: 4961 (Introduction, Methods, Results, Discussion)

Total number of figures and tables: 5 main figures, 8 supplementary figures

Abstract

Acute myeloid leukemia (AML) is a genetically heterogeneous, aggressive hematological malignancy induced by distinct oncogenic driver mutations. The effect of specific AML oncogenes on immune activation or suppression has not been

investigated. Here, we examine immune responses in genetically distinct models of AML and demonstrate that specific AML oncogenes dictate immunogenicity, the quality of immune response and immune escape through immunoediting. Specifically, expression of $Nras^{G12D}$ alone is sufficient to drive a potent anti-leukemia response through increased MHC Class II expression that can be overcome with increased expression of Myc. These data have important implications for the design and implementation of personalized immunotherapies for patients with AML.

Statement of Significance

The endogenous immune response against acute myeloid leukemia (AML) is determined by leukemia-specific oncogenic driver mutations. Mutant Nras drives immunological selection of AML.

Introduction

Acute myeloid leukemia (AML) is caused by the acquisition of genetic mutations in hematopoietic stem and progenitor cells (HSPCs) resulting in a block in myeloid differentiation and the expansion of immature myeloid blasts [1]. AML is genetically heterogeneous with recurrent genetic abnormalities resulting in activation of signal transduction pathways, impaired function of lineage specific transcription factors and dysregulation of epigenetic modifiers [2]. Survival and response to chemotherapy is dependent on the age and molecular profile of AML patients [3, 4]. Despite chemotherapy, followed where possible by allogeneic hematopoietic stem cell transplantation (allo-HSCT), or low-intensity combination therapies for elderly

patients [5], long-term survival is less than 50% overall and is attributed to relapse or therapy resistance highlighting the importance of developing novel therapies.

There is increasing evidence to support a functional interaction between AML and the immune system [6, 7]. AML patients exhibit myeloid dysfunction, cytotoxic lymphocyte dysfunction of both NK and T cells, secretion of suppressive molecules and upregulation of immune suppressive ligands on AML cells [8-13]. Studies indicate that immune microenvironment composition is also important for response to chemotherapeutic treatments. For example, AML patients with abnormal NK cell function and downregulation of NK cytotoxicity surface receptors have defective NK clearance of leukemic blasts [14-17]. Lymphocyte recovery after chemotherapy is associated with improved survival and there are even rare cases of spontaneous remission after severe infections [18, 19]. Early clinical trials suggest that combining hypomethylating agents and immune checkpoint inhibitors may have efficacy in AML, however these results have not yet been confirmed in randomized studies [20, 21]. AML has a low somatic mutation burden and is predicted to have a low frequency of potential neoantigens [22, 23]. This poses the question, what regulates immune responses in AML and can distinct genetic aberrations influence immunogenicity? Characterization of the immune microenvironment in specific types of AML, including the mechanisms of immune escape, may help to understand whether the endogenous immune response is capable of controlling, or eliminating AML.

We have investigated the immunogenicity of genetically distinct models of AML, representing common clinical and prognostic subsets of genetic alterations found in

AML patients [24, 25]. We found that distinct oncogenes altered the host immune response to the leukemia and that mutant Nras was a key determinant of this immunological selection [26, 27].

Altogether, these data provide new insights into a hitherto unrecognized endogenous immune response in AML and generate a path for the strategic use of immunotherapies for subsets of AML patients.

Materials and Methods

Murine AML models

AML from primary hematopoietic stem and progenitor cells (HSPC) were generated as previously described [28-30], see supplementary methods. Wild type C57BL/6J mice were purchased from ARC Animal Resources Centre or Walter and Eliza Hall Institute for Medical Research. Rag2$^{-/-}$γc$^{-/-}$(Rag2$^{-/-}$ Il2rg$^{-/-}$) were back-crossed onto C57BL/6J. Pathogen-free mice were maintained with approval by QIMR Berghofer institutional ethics committee protocol A11605M, A1212-619M and A1212-620M. Npm1c-Nras^{G12D} AML cells, generated as previously described [31], were obtained from Prof. Wallace Langdon (UWA) and Prof. George Vassiliou (Wellcome Sanger Institute).

In vivo antibody experiments

In vivo antibody depletion in wild type mice was performed using the following antibodies: anti-CD4 (100 μg, GK1.5; Bio-X-Cell), anti-CD8β (100 μg, 53.5.8; Bio-X-

Cell) and control IgG (100 μg, HRPN; Bio-X-Cell). Antibodies were injected into the intraperitoneal cavity on days -1 and 0 and then weekly for the duration of the experiment. Anti-PD-1 (250 μg, RMP1-14, Bio-X-Cell) immune checkpoint inhibitor experiments commenced 7 days after transplant, with treatment every 3-4 days, with a total of 9 doses administered.

T cell Proliferation assay

Non-irradiated wild type C57BL/6J mice were transplanted with $Nras^{G12D}$ or MA9 AML previously expanded in $Rag2^{-/-}\gamma c^{-/-}$ mice. Whole splenocytes were harvested, labeled with Cell Trace Violet (CTV) and incubated for 72 hours at a 5:1 ratio with and without irradiated (40Gy) $Nras^{G12D}$, MA9 (passaged through $Rag2^{-/-}\gamma c^{-/-}$ mice) or non-transformed $Rag2^{-/-}\gamma c^{-/-}$ bone marrow (BM) cells and 0.01μg/mL soluble CD3 (2C11, Biolegend). Dilution of CTV on CD4+ and CD8+ T cell populations was evaluated by flow cytometry. The proliferation indexes of CD4+ and CD8+ T cells were calculated by dividing the total number of divisions by the number of cells that underwent division.

Blood analysis

Blood collected into EDTA-coated tubes was analyzed on a Hemavet 950 analyser (Drew Scientific).

Fluorescence activated cell sorting and analysis (FACS)

Spleens and livers were harvested into ice cold FACS buffer (PBS supplemented with 2% FCS v/v) and then emulsified through a 70μM filter (BD Biosciences),

centrifuged and washed in FACS buffer. Liver mononuclear cells were isolated using isotonic percoll gradient. Tissue samples were treated with Red Blood Cell Lysis Buffer (BD Pharmlyse, BD Biosciences). Samples were incubated in CD16/CD32 blocking antibody (clone 93; Biolegend) before staining with appropriate fluorochrome-conjugated antibodies as indicated (Supplementary Table 1). Post-acquisition analyses were performed using FlowJo software V10.0 (Treestar, CA). Cell analysis and sorting were performed using the BD FACS LSR Fortessa^{TM} or BD FACSAria^{TM}.

RNA-sequencing analysis

GFP positive AML cells were isolated on BD FACSAria^{TM}, washed in ice cold PBS including 1:500 protease inhibitor cocktail (Sigma Aldrich) prior to snap freezing on dry ice. Total RNA was isolated from frozen cell pellets using the Arcturus PicoPure RNA Isolation Kit (Applied Biosystems). Samples were quantitated using a Qubit RNA HS Assay Kit (Molecular Probes), with integrity confirmed using the RNA 6000 PICO Kit (Agilent Technologies) and Agilent 2100 Bioanalyser (Agilent Technologies).

Quantitative Polymerase chain reaction (qPCR)

DNase free RNA was extracted from sorted GFP+ Nras^{G12D} cells using Arcturus PicoPure RNA Isolation Kit (Applied Biosystems) according to the manufacturer's instructions. Reverse transcription was performed using Maxima H minus first strand cDNA synthesis kit with dsDNase according to the manufacturer (Thermofisher Scientific). Genomic DNA was extracted using QIAGEN DNeasy Blood and Tissue

kit according to the manufacturer's instructions. RNA and DNA quantification concentration and purity were determined by Nanodrop spectrophometer (ThermoFisher Scientific). Q-PCR primers were designed using Primer2web (http://bioinfo.ut.ee/primer3/).

Statistical and Bioinformatics analysis

Statistical analysis was performed using Prism (v7.02) as follows: Log-rank (Mantel-Cox) test for p values for all Kaplan-Meier survival analyses. To compare two groups unpaired Student's t-test when normality and equal variance assumptions are met, Mann-Whitney test otherwise; unless otherwise described for more than two groups when normal distribution and equal variance assumption are met ordinary one-way ANOVA with post-Tukey multiple comparison test was performed, in case of violation of equal variance we performed Welch ANOVA or Kruskal-Wallis test with Dunn's multiple comparisons test when normality is violated. Test for association between paired samples, using Pearson's product moment correlation coefficient. Detailed bioinformatics protocols are provided in Supplementary methods.

Data Availability

All RNA sequencing datasets generated in this study are available through NCBI Gene Expression Omnibus under accession numbers GSE164951 and GSE207316. Publicly availably AML microarray data used in this study have the accession number GSE6891. Publicly available AML and healthy single cell CITE and RNAseq data have the accession number GSE185381. Further information and requests for

187 resources and reagents should be directed to, and will be fulfilled by, Steven Lane

188 (steven.lane@qimrberghofer.edu.au).

189

190

Results

Oncogene specificity defines AML immune response

We generated three genetically distinct models of AML; NUP98-HOXA9+BCR-ABL (BA/NH), MLL-AF9 (MA9) or AML1-ETO/Nras^{G12D} (AE/Nras^{G12D}), representative of common genetic alterations found in patients with AML [3] (Fig. 1A). Rag2$^{-/-}$γc$^{-/-}$ donors were used to avoid the transfer of mature lymphoid immune cells from the donor graft [32]. Rag2$^{-/-}$γc$^{-/-}$ and wild-type C57BL/6J (WT) had similar HSPC baseline function assessed by colony formation in cytokine enriched methylcellulose (Supplementary Fig. S1A) [1]. Primary (1º) AML developed in all recipients reconstituted with AML oncogene-expressing BM (Supplementary Fig. S1B) but not with HSPCs transduced by retrovirus without oncogene expression. AML generated from the dual transduction of oncogenes were genotyped to confirm the integration of both vectors (Supplementary Fig. S1C).

In order to determine the effect of the immune system on disease progression, 1º AMLs were transplanted into secondary (2º) non-irradiated immunodeficient Rag2$^{-/-}$ γc$^{-/-}$ or immunocompetent WT recipients (Fig. 1B-G). BA/NH induced AML in either WT or Rag2$^{-/-}$γc$^{-/-}$ recipients with similar overall survival (Fig. 1B and E, Supplementary Fig. S1D). In contrast, MA9 AML and AE/Nras^{G12D} AML progressed more rapidly in Rag2$^{-/-}$γc$^{-/-}$ compared to WT recipients (Fig. 1C-D and F-G, Supplementary Fig. S1E and S1F) with AE/Nras^{G12D} AML showing the most prolonged latency in immunocompetent hosts. BM AML engraftment was similar between Rag2$^{-/-}$γc$^{-/-}$ and WT at 24hrs post-transplant indicating similar homing to BM (Supplementary Fig. S1G). Furthermore, extending disease latency in BA/NH AML

with the transplantation of fewer cells did not increase disease latency in WT recipients in comparison to Rag2$^{-/-}$γc$^{-/-}$ (Supplementary Fig. S1H). These data indicate a graded immune response to AML subtypes that is specified by individual oncogenes.

Oncogene specificity influences mediators of immune recognition and immune activity

We next determined if the differences in AML immunogenicity are reflected through cell intrinsic differences in the expression of cell surface immune recognition markers by comparing the immunophenotype of the genetically distinct AMLs maintained exclusively in immunodeficient Rag2$^{-/-}$γc$^{-/-}$ recipients. Analysis restricted to the AML CD11b+ myeloid population (Supplementary Fig. S2A) showed that AE/Nras^{G12D} was characterized by the highest expression of antigen presentation machinery, H2-D^{b}, H2-K^{b} and MHC Class II (Fig. 2A, Supplementary Fig. S2B). Unexpectedly, after serial transplantation the AE/Nras^{G12D} AML passaged in both the Rag2$^{-/-}$γc$^{-/-}$ and WT 2^{o} recipients only retained integration of the Nras^{G12D} construct (hereafter referred to as Nras^{G12D}) (Supplementary Fig. S2C). Consistent with this, analysis of Rag2$^{-/-}$γc$^{-/-}$ HSPCs at 72hrs post transduction with the individual oncogenes, demonstrated that acute expression of Nras^{G12D} alone was sufficient to drive increased surface expression of MHC Class II (Supplementary Fig. S2D). These findings were further confirmed using microarray data of bulk AML samples at diagnosis from 42 patients with an NRAS mutation compared to 10 patients with an MLL translocation (MLL-X). Here, NRAS mutant human AML showed increased expression of multiple HLA

(MHCII) genes, including HLA-DQA1, compared to MLL-X translocated AML (Fig. 2B, Supplementary Fig. S2E). Using single sample gene set enrichment, MHCII score was associated with AML patients driver mutations and chromosomal aberrations [33], with NRAS mutant patients ranked as one of the highest MHCII expressing genetic groups while MLL-X translocated patients rank among the lowest (Fig. 2C). Single cell RNA-sequencing demonstrated that malignant CD33-expressing AML blasts from RAS mutant patients maintained MHCII gene expression, whereas malignant CD33-expressing blasts from MLL-X AML patient samples had reduced expression in comparison to healthy CD33-expressing BM (Fig. 2D).

Next, we examined the difference in the expression of discrete panel of immunomodulatory cell surface molecules in murine AML samples. We found that $Nras^{G12D}$ AML was characterized by the highest expression of the CD28 ligands, CD80 and CD86 (Fig. 2E, Supplementary Fig. S3A). Conversely, BA/NH had high expression of the immunosuppressive ligands PD-L1 and GAL-9 and CD155 (Fig. 2E, Supplementary Fig. S3A). Analysis of $Rag2^{-/-}\gamma c^{-/-}$ HPSCs at 72hrs post transduction with the individual oncogenes, demonstrated that acute expression of $Nras^{G12D}$ alone is sufficient to drive increased surface expression of CD80 and CD86 (Supplementary Fig. S3B). Conversely, neither acute expression of BCR-ABL nor NUP98-HOXA9 alone was sufficient to increase PD-L1, GAL-9 or CD155 (Supplementary Fig. S3B).

We next sought to determine if evidence of an anti-AML immune response was present in a genetically engineered knockin model of mutant Nras-driven AML,

derived from mice heterozygous for conditional alleles conferring a C-terminal truncation in Npm1 and constitutively active Nras (*Tg(MxI-cre), Npm1$^{fl\text{-}cA/+}$; Nras$^{fl\text{-}G12D/+}$*), expressed from their respective endogenous promoters [31]. We expanded the AML by transplantation into immunodeficient mice and then transplanted this AML into tertiary (3^{o}) non-irradiated immunodeficient Rag2$^{-/-}$γc$^{-/-}$ or immunocompetent WT recipients. Npm1c-Nras^{G12D} AML cells generated a rapid, fully penetrant AML when transplanted into Rag2$^{-/-}$γc$^{-/-}$ recipients, however there was a marked delay in disease latency in immunocompetent WT recipients (Fig. 2F-G), confirming an intrinsic immune response to a genetically engineered AML mouse model driven by mutant Nras.

These data reveal discrete effects of oncogenic drivers on immune regulatory molecule expression in AML cells, supporting a model whereby Nras^{G12D} AML has greater potential to interact with the immune system.

Oncogene specificity determines the composition of the AML immune microenvironment

Given the role of MHC, CD80 and CD86 in T cell activation, we compared the requirement for T cells in controlling disease progression in MA9 and Nras^{G12D} AML. WT recipient mice were treated with isotype control, or antibodies that depleted T cells (CD4 and CD8). Immune cell depletion was verified in the peripheral blood (Supplementary Fig. S4A). In Nras^{G12D}, depletion of T cells accelerated the development of AML (Fig. 3A). Similar findings were observed in the MA9 model but

this effect was much less pronounced (Fig. 3B). Consistent with a specific T cell mediated immune response, we demonstrated that $Nras^{G12D}$ AML ($Rag2^{-/-}\gamma c^{-/-}$) increases T cell proliferation upon co-culture in comparison to non-transformed BM ($Rag2^{-/-}\gamma c^{-/-}$) whereas MA9 AML did not (Fig 3C-D).

We next sought to determine if this differential requirement for T cells in the anti-leukemic response was reflected in the composition of the immune microenvironment. We observed a significant decrease in the frequency of T cells within the microenvironment of the leukemia-bearing spleens of BA/NH recipients compared to MA9 and $Nras^{G12D}$ recipients and naïve controls (Fig. 3E). We note that the BA/NH recipients demonstrated complete effacement of splenic architecture concordant with this loss of normal T-cell populations. Within T cells, $Nras^{G12D}$ recipients display the lowest percentage of CD4+ T cells and subsequently the highest frequency of CD8+ T cells (Fig. 3E). Interestingly, all AML recipients display contraction in the proportion of naïve CD4+ and CD8+ cells (CD44-CD62L+), an expansion in CD4+ and CD8+ T effector memory (CD44+CD62L-) and a decrease in CD4+ and CD8+ T central memory (CD44+CD62L+) formation when compared to naïve controls (Fig. 3E, Supplementary Fig. S4B-D). Of note however, is that BA/NH recipients retain the greatest frequency of naïve CD8+ T cells, with $Nras^{G12D}$ recipients having a greater frequency of CD8+ T effector memory compared to BA/NH recipients (Fig. 3E, Supplementary Fig. S4D).

As these immunocompetent recipients were analyzed after developing AML, we compared the impact of AMLs driven by distinct oncogenic drivers on markers of CD4+ and CD8+ T cell activation and dysfunction. There was an increase in the

frequency of PD-1+/DNAM-1+ CD4+ and CD8+ T cells in AML recipients compared to naïve spleen, indicating an expansion of effector T cells with reduced cytotoxic potential (Fig. 3F, Supplementary Fig. S5A-D). However, the co-expression of co-inhibitory receptors KLRG1 and PD-1 was significantly increased on CD4+ and CD8+ T cells from Nras^{G12D} recipients only compared to naïve spleen (Fig. 3F, Supplementary Fig. S5A-D). Finally, co-expression of PD-1 and TIM-3, indicating a T cell exhaustion phenotype, was increased on CD4+ and CD8+ T cells from Nras^{G12D} recipients, but was only increased on the CD4+ T cells in BA/NH recipients and not increased on T cells from MA9 AML (Fig. 3F, Supplementary Fig. S5A-D). We sought to validate these murine findings in human AML using single cell RNA-sequencing analysis. Consistent with the murine findings, we observed that greater frequency of T cells isolated from the bone marrow of mutant RAS AML patients demonstrated PD-1 gene expression in comparison to those isolated from MLL-X translocated AML patients (Fig. 3G). These data indicate expansion and dysfunction of the effector T cell compartment as a distinguishing feature of the immune microenvironment of immunogenic AML.

Immunoediting selects against immunogenic AML

Despite a robust immune response that delayed AML onset, MA9 and Nras^{G12D} leukemias were eventually able to develop in the presence of a competent immune system. We hypothesized that this immune escape could be mediated through immunoediting, the selection of disease with decreased immunogenicity [26, 27] or via immunosuppressive effects on the host immune system. To functionally examine for immunoediting, we compared the disease latency of AML passaged through

328 immunocompetent mice vs. AML passaged through immunodeficient mice when
329 these were transplanted into either an immunocompetent WT or immunodeficient
330 Rag2$^{-/-}$γc$^{-/-}$ recipients (Fig. 4A). For both leukemias, there was no difference in
331 disease latency when transplanted into Rag2$^{-/-}$γc$^{-/-}$ mice, suggesting that passage
332 through an immunocompetent host does not change the proliferative capacity of
333 these AMLs (Fig. 4B). However, there was accelerated disease progression in
334 immunocompetent mice transplanted with Nras^{G12D} AML that had been previously
335 passaged through immunocompetent WT mice (2^{o} WT; 3^{o} WT), compared to AML
336 passaged previously through immunodeficient Rag2$^{-/-}$γc$^{-/-}$ mice (2^{o} Rag2$^{-/-}$γc$^{-/-}$; 3^{o}
337 WT) (Fig. 4B). In contrast, disease latency in immunocompetent mice was
338 unchanged for MA9 AML, regardless of whether the AML was previously passaged
339 through immunocompetent (2^{o} WT; 3^{o} WT) or immunodeficient (2^{o} Rag2$^{-/-}$γc$^{-/-}$; 3^{o}
340 WT) mice, suggesting that immunoediting is not observed in MA9 AML (Fig. 4C) and
341 reflecting the more immunogenic phenotype of Nras^{G12D} (Fig. 1F-G). This
342 demonstrates that Nras^{G12D} AML is immunoedited during passage through
343 immunocompetent recipients.

344 Given the elevated expression of a number of immune regulatory molecules of the
345 surface of Nras^{G12D} AML (Fig. 2A, D and Supplementary Fig. S2B and S3A), we
346 used flow cytometry to examine the immunophenotype of non-immunoedited versus
347 immunoedited Nras^{G12D} cells (Supplementary Fig. S6A). Surprisingly, we didn't
348 observe any difference in the abundance of H-2D^{b} and MHC Class II, and only a
349 minor increase in H-2K^{b} (Fig. 4D). In contrast, we saw the upregulation of ligands
350 with potential immunosuppressive function, PD-L1 and CD86 (Fig. 4E). These

findings suggest that immunoedited Nras^{G12D} AML may suppress the anti-leukemic immune response to facilitate disease progression.

As PD-L1 interacts with the immune-suppressive receptor PD-1 on T cells, we determined whether blockade of the PD-1/PD-L1 interaction with anti-PD-1 was able to reactivate an anti-leukemic immune response in immunoedited Nras^{G12D} AML (Fig. 4F). We observed minor, but significant effects on AML control after anti-PD-1 antibody treatment. Anti-PD-1 treated mice showed a lower penetrance of AML infiltration in the liver, the major site of infiltration of this disease in unconditioned immunocompetent mice, with fewer tumors per liver and a trend to reduced tumor area (Fig. 4G). These data demonstrate that restoring immune cell function through anti-PD-1 treatment can facilitate anti-leukemic control, but has limited efficacy in established disease when used as a single agent. This is consistent with published data showing only a modest effect of PD1 blockade in MDS and AML [20].

As modulating the surface immune checkpoints were insufficient to reinstate immunoedited Nras^{G12D} AML, we used RNA-sequencing to investigate transcriptional changes between non-immunoedited and immunoedited Nras^{G12D} AML (Supplementary Fig. S6A-B, Supplementary Table 1). Surprisingly, the gene expression of immunoedited AMLs showed evidence of pathway down-regulation for NRAS signaling (Fig. 5A, Supplementary Table 1), correlating with decreased gene expression of Nras compared to non-immunoedited cells (Supplementary Fig. S6C-D, Supplementary Table 1). Q-RT-PCR analysis of genomic DNA of non-immunoedited and immunoedited Nras^{G12D} cells revealed that immunoediting selected for cells with reduced Nras^{G12D} copy number (Fig. 5B). Furthermore, the

374 immunoedited AMLs were characterized by the increased expression of targets of
375 MYC, a transcription factor conventionally considered to have a master regulatory
376 role in growth and proliferation (Fig. 5C, Supplementary Table 1). Nras^{G12D} AML in
377 WT secondary recipients showed only a slightly higher frequency of Ki67 positive
378 cells, with no difference in the mitotic marker phosho-Histone H3 (Supplementary
379 Fig. S6E-F). Consistent with this finding, transplant of equal numbers of non-
380 immunoedited and immunoedited Nras^{G12D} cells into immunodeficient Rag2$^{-/-}$γc$^{-/-}$
381 mice generated disease with comparable latency suggesting that no intrinsic
382 differences in proliferative capacity occurred as a consequence of immunoediting
383 (Fig. 4B). Importantly, changes in NRAS and MYC gene sets were not observed
384 when comparing MA9 AML passaged through WT vs Rag2$^{-/-}$γc$^{-/-}$ recipients
385 (Supplementary Fig. S6G, Supplementary Table 1). However, we did observe that
386 MA9 AMLs exposed to a competent immune environment upregulated the
387 expression of genes involved in interferon signaling and that this did not occur in the
388 immunoedited Nras^{G12D} AML (Supplementary Fig S6G-I, Supplementary Table 1).
389 These data indicate that immunoediting in Nras^{G12D} AML may involve coordinate
390 clonal selection for cells with reduced mutant Nras expression and increased Myc-
391 driven transcription to evade immune control.

392

393 **Ectopic expression of Myc reduces immunogenicity in Nras^{G12D}-driven AML**

394 There is increasing evidence that MYC is a critical determinant of an
395 immunosuppressive tumor microenvironment and that MYC inactivation enables
396 recruitment of lymphocytes into tumors [34-37]. Consistent with this, in NRAS-mutant

AML, we observed that a tissue-agnostic set of Myc transcriptional targets showed an inverse correlation with a predictive gene signature of cytotoxic immune cell infiltration in AML (Fig. 5D, Supplementary Table 2) [38, 39].

To functionally examine the consequence of elevated Myc expression on immune evasion in AML, we generated $Nras^{G12D}$ AML expressing ectopic levels of Myc in comparison to an empty vector (EV) control. Dual oncogene integration was confirmed by expression of both GFP ($Nras^{G12D}$) and mCherry (Myc) fluorescent markers. Ectopic Myc expression resulted in only minor differences in MHC Class I surface expression ($H2\text{-}D^b$ and $H2\text{-}K^b$), but a marked increase in PD-L1 and CD86 expression (Fig. 5E). Unexpectedly, ectopic Myc also resulted in a striking reduction in MHC Class II surface expression.

In order to functionally assess the effect of ectopic Myc expression on the anti-AML immune response in vivo, we transplanted both the $Nras^{G12D}$/Myc and $Nras^{G12D}$/EV AMLs into both immunodeficient and immunocompetent recipients. Ectopic Myc expression resulted in slightly accelerated disease progression in the $Rag2^{-/-}\gamma c^{-/-}$ recipients, and this difference was dramatically increased in immunocompetent recipients. Combined, this data supports the conclusion that increased expression of Myc results in reduced immunogenicity in $Nras^{G12D}$-driven AML.

Discussion

The role of the host immune system in controlling certain cancers is well established, but data are lacking in the context of AML. Here, we have used genetically distinct murine models of AML to investigate oncogene-dependent immunogenicity of AML

cells. These included BA/NH, a myeloid blast-crisis model with poor prognosis; MA9, aberrant activity of epigenetic modifier; and, AE/Nras^{G12D} and Npm1^{mutant} /Nras^{G12D} AML, the latter two genotypes are associated with a favorable prognosis after treatment. We present evidence that the immunogenicity of AML cells and the quality of the immune response are directed by the specific oncogenic driver that induces the AML.

Of the oncogenic drivers tested, the strongest immune response was induced by Nras^{G12D}, evidenced by the greatest difference in disease latency between immunodeficient and immunocompetent mice. We found distinct expression levels of antigen presentation machinery and inhibitory and activating immune cell ligands on the different AMLs in the absence of exposure to a competent immune system. Furthermore, we found that immune cell ligand expression corresponds to the observed difference in AML immunogenicity, indicating that oncogenes influence the inherent potential of an AML cell to interact with the immune system. Specifically, BA/NH cells had low expression of MHC Class I (H2-D^{b} and H2-K^{b}) together with high expression of inhibitory immune checkpoint ligands PD-L1, GAL-9 and CD155 compared to MA9 and Nras^{G12D}. This indicates that the non-immunogenic phenotype of BA/NH may be driven by inherent low antigen presentation and high expression of immune suppressive checkpoint molecules. In contrast, Nras^{G12D} cells displayed a different cell surface phenotype with increased expression of antigen presentation machinery and immune-stimulatory ligands. Indeed, when we looked across a more extensive panel of molecular subtypes, RAS mutant human AML demonstrates high HLA Class II expression. It must be noted that MA9 AML exhibited an appreciable immunogenic phenotype despite exhibiting low levels of MHC Class I and II

443 expression, suggesting a possible role for other immune cells such as NK cells in the
444 control of this leukemia.

445 Expression of the HLA Class II presentation machinery has recently been suggested
446 as a determinant of immune evasion in hematological malignancies [39]. It has been
447 shown that HLA Class II expression in AML is in part dependent on the methylation
448 status of the promoter of the transcriptional coactivator CIITA, and its expression,
449 which is IFNγ responsive [39]. Interestingly, the expression of the co-stimulatory
450 molecule CD80 is also IFNγ responsive [40] and mutant Ras has recently been
451 shown to drive a cell-intrinsic interferon response via increased expression of
452 transposable elements [41] providing a possible mechanism for the unique surface
453 immunophenotype of the immunogenic $Nras^{G12D}$ AML. This also poses the
454 interesting hypothesis as to whether AML immunogenicity can be enhanced by the
455 administration of IFNγ, either alone or in combination with hypomethylating agents.

456 Consistent with the hypothesis that cell intrinsic differences in AML surface
457 expression of immunomodulatory ligands dictate the potential for an anti-leukemia
458 immune response, individual genetic aberrations also dictate the composition of the
459 tumor microenvironment, including the degree of myeloid and lymphocyte cell
460 infiltration and dysfunction [42]. We identified distinct oncogene-dependent immune
461 microenvironments in AML recipient immunocompetent mice. Expansion of CD8+
462 effector T cells in $Nras^{G12D}$ recipients indicates activation of the adaptive immune
463 response that was observed to a much lesser extent in BA/NH or MA9 recipients.
464 This was consistent with depletion experiments demonstrating a more dominant role
465 for T cells in control of $Nras^{G12D}$ in comparison to MA9 AML. Furthermore, a higher

466 frequency of CD8+ T cells in the Nras^{G12D} AML microenvironment of moribund mice
467 displayed expression of immunosuppressive receptors PD-1 and TIM-3. Consistent
468 with this, examination of T cells from AML patients at diagnosis also revealed that a
469 higher frequency of T cells in the RAS mutant AML tumor microenvironment display
470 gene expression of PD-1 in comparison to MLL translocated AML, suggesting that
471 RAS mutant AML can only progress in the context of inhibitory receptor expression
472 on T cells.

473 In addition to immune dysfunction, immune evasion may also be facilitated by
474 immunoselection against the most immunogenic tumor cells, a dynamic process
475 referred to as immunoediting [26, 27] and can be mediated by T cell-dependent
476 selection against immunogenic neo-antigens and IFNγ associated genetic instability
477 [43-45]. Here, the more immunogenic Nras^{G12D} AML showed functional
478 immunoediting in immunocompetent mice whereas the less immunogenic MA9 AML
479 did not, possibly reflecting the difference in the efficacy of T cells in controlling these
480 AMLs. Immunoediting has been described in mouse sarcoma models [46], but to our
481 knowledge, this is the first experimental validation of functional immunoediting in a
482 syngeneic AML model. The different capacities for immunoediting presumably reflect
483 the strength of the effector immune cell response and the degree of *in vivo* selective
484 pressure. Immunoediting is also seen in highly selective clinical settings, specifically
485 after the use of CD20-directed monoclonal antibodies and CD19-directed CAR-T cell
486 therapy for ALL where CD20 and CD19 negative relapses are observed and facilitate
487 escape from CAR-T cell killing [47, 48]. Further evidence of immunoediting is seen in
488 AML relapse after allogeneic BM transplantation which is frequently associated with

489 downregulation of HLA Class II molecules [11, 49] or polymorphisms in the HLA
490 region [50].

491 Although immunoediting was characterized by the upregulation of the
492 immunosuppressive ligand PD-L1, anti-PD1 therapy had limited efficacy in restoring
493 the anti-leukemia immune response in this model, suggesting that the strategy
494 employed in the immunoedited $Nras^{G12D}$ AML to evade the immune system is likely
495 to be multifaceted. While ICB clinical trials are ongoing in AML patients, preliminary
496 data suggests that single agent ICB also has minimal activity in AML patients
497 whereas ICB in combination with hypomethylating agent azacitidine has shown
498 positive responses in a proportion of AML patients with higher pretherapy bone
499 marrow CD3+ and the presence of ASXL1 mutation, again suggesting that patient
500 genetic profiles are important predeterminants of treatment efficacy [20, 51].

501 We hypothesize that immunoediting in $Nras^{G12D}$ AML is driven by the coordinate
502 downregulation of mutant Nras expression and upregulation of Myc-driven
503 transcription. The down regulation of mutant Nras expression is consistent with the
504 immunogenicity of this AML being in part driven by the presentation of immunogenic
505 neo-antigens generated from mutant Nras. Our data are supported by previous
506 studies in mouse models of sarcoma, that identified T cell-dependent
507 immunoselection driving immunoediting against highly antigenic neo-epitopes
508 derived from specific genetic mutations [43, 44]. KRAS mutant-specific T cells have
509 been found in melanoma patients showing that the immune system is capable of
510 directly targeting mutant RAS derived neo-antigens [52] and the presence of NRAS
511 mutations may confer better response rates to immune checkpoint therapy [53]. RAS

mutant AML has a relatively favorable prognosis after treatment with chemotherapy. It could be hypothesized that this may relate to the presence of a host immune response, and that this response can be unmasked after tumor de-bulking through chemotherapy.

There is increasing evidence showing that MYC is a critical modulator of an immunosuppressive tumor microenvironment and that MYC inactivation enables recruitment of lymphocytes into tumors [34-37]. Consistent with this, we found that MYC transcriptional activity AML inversely correlates with the presence of a cytolytic immune infiltrate. We have demonstrated that the ectopic expression of Myc alone is able to reduce surface expression of both MHC Class I and II in non-immunoedited $Nras^{G12D}$ AML, in addition to driving the increased surface expression of PD-L1 and CD86. MYC activity has previously been implicated in regulating both transcription and translation of PD-L1 [37, 54]. However, we believe this is the first time that Myc activity has been linked to the expression of antigen presentation machinery. Interestingly, recent studies have described a direct role for Myc in the repression of interferon response genes in $Nras^{G12D}$ driven models of pancreatic ductal adenocarcinoma and triple negative breast cancer [55, 56]. It is tempting to speculate that Myc-mediated suppression of mutant RAS driven activation of interferon signaling may be an unappreciated aspect of this cooperative oncogenic relationship that is exploited by cancers of all cell lineages.

In summary, these data point to anti-leukemic immune responses being determined by specific oncogenic profiles. Critically, in the case of $Nras^{G12D}$, extrinsic immune pressure enables outgrowth of less immunogenic AML cells. $Nras^{G12D}$ shows

535 transcriptional plasticity under immune selective pressure, and may undergo
536 changes in gene and surface marker expression resulting in upregulation of an
537 immunosuppressive phenotype. As immunotherapy approaches undergo clinical
538 testing in myeloid blood cancers, these findings highlight that personalized and
539 targeted treatment plans may be designed according to the genetics of AML
540 patients.

541

542 **Acknowledgements**

543 We are grateful for the assistance of the QIMR Berghofer animal house, flow
544 cytometry, microscopy and histology facilities and helpful comments from members
545 of the Lane Lab and Immunology Department at QIMR Berghofer Medical Research
546 Institute. Specifically, Mark Smyth for his extremely valuable intellectual contributions
547 and assistance with reagents, Rachel Kuns for help generating MHC Class II
548 knockout AML and Madeleine Headlam and Keyur Dave for proteomics service and
549 analysis. We thank Thomas Mercher for helpful comments and review of the
550 manuscript.

551 We gratefully acknowledge the support of the Herron Family Trust, CSL Centenary
552 Fellowship (SWL), NHMRC (Ideas Grant 2003575), Gordon and Jessie Gilmour
553 Fellowship and Leukaemia Foundation of Australia (RA). CB and human AML work
554 were supported by NHMRC Project Grant (1157263). MB was supported by a
555 fellowship of the Mildred-Scheel Stiftung fur Krebsforschung (Germany). FSFG was

556 supported by a NHMRC Early Career Fellowship (1088703), a National Breast
557 Cancer Foundation (NBCF) Fellowship (PF-15-008).

558 Figures and Figure legends

559 **Figure 1: Oncogene specificity dictates AML immunogenicity.** (A) Schema for
560 *in vivo* generation of oncogene-specific retroviral 1° AMLs in Rag2$^{-/-}$γc$^{-/-}$ mice, then
561 passaged through 2° Rag2$^{-/-}$γc$^{-/-}$ or wildtype (WT) C57BL/6J mice. Peripheral blood
562 (PB) leukemic burden (WBC x GFP %) of secondary recipients: (B) BA/NH day 12
563 post-transplant, (C) MA9 day 16 post-transplant, (D) AE/Nras^{G12D} on day 20 post-
564 transplant. Data from one of two repeat experiments. Kaplan-Meier curves
565 comparing survival between Rag2$^{-/-}$γc$^{-/-}$ and WT secondary recipients transplanted
566 with 150,000 1° AML cells demonstrating (E) BA/NH (Rag2$^{-/-}$γc$^{-/-}$ n = 4; WT n = 5;
567 median survival 14 days), (F) MA9 (Rag2$^{-/-}$γc$^{-/-}$ n = 10; WT n = 10; median survival 18
568 vs. 25 days respectively) and, (G) AE/Nras^{G12D} (Rag2$^{-/-}$γc$^{-/-}$ n = 10; WT n = 10;
569 median survival 22 vs. 95 days respectively). BA/NH demonstrating data from one
570 experiment. MA9 and AE/Nras^{G12D} demonstrating pooled data from two experiments.
571 Each point represents a biological replicate. Mann-Whitney test for comparison
572 between two groups and Mantel-Cox test for comparison of Kaplan-Meier curves. * p
573 <0.05, ** p < 0.01, *** p <0.001, **** p <0.0001.

574 **Figure 2: Oncogene specificity influences the immunogenicity of AML cells.** (A)
575 Median fluorescence intensity (MFI) of H2-D^{b}, H2-K^{b}, MHC Class II (IA/E) on cell
576 surface of myeloid cells (CD11b+) from bone marrow (BM) of naïve wildtype mice
577 and GFP+ CD11b+ BA/NH, MA9 and Nras^{G12D} AML cells in the spleens of Rag2$^{-/-}$γc^{-}
578 $^{/-}$ recipients moribund with disease. Each point represents a biological replicate

derived from independent mice transplanted with the same tumor. (B) Microarray derived gene expression of HLA-DQA1 from bulk PB/BM of 10 MLL-translocated (MLL-X) and 42 Nras mutant AML patients [33] (C) MHCII ssGSEA across Verhaak dataset genotypes (D) HLA-DQA1 gene expression in malignant CD33-expressing AML blasts derived from single cell RNA-sequencing of BM from patients with a MLL-X AML or a mutant RAS AML in comparison to CD33-expressing cells from healthy bone marrow [57]. (E) MFI of CD80, CD86, PD-L1, GAL-9 and CD155 on cell surface of myeloid cells (CD11b+) from BM of naïve wildtype mice and GFP+ CD11b+ BA/NH, MA9 and $Nras^{G12D}$ AML cells in the spleens of $Rag2^{-/-}\gamma c^{-/-}$ recipients moribund with disease. (F) Kaplan-Meier curves comparing survival between $Rag2^{-/-}\gamma c^{-/-}$ and wildtype (WT) recipients transplanted with equal numbers of AML cells derived from a moribund *Tg(Mx1-cre), $Npm1^{fl\text{-}cA/+}$; $NRas^{fl\text{-}G12D/+}$ mouse* (Npm1c/$Nras^{G12D}$)[31]. (G) WBCC of mice transplanted with Npm1c-$Nras^{G12D}$ AML when moribund ($Rag2^{-/-}\gamma c^{-/-}$) or 63 days post-transplant (WT). Each point represents a biological replicate derived from independent mice transplanted with the same tumor. One-way ANOVA (C) with Tukey's multiple testing correction (A: H2-D^b, H2-K^b), E: CD80, CD86)), Mann-Whitney test for pairwise comparisons between groups (B), Kruskal-Wallis test with Dunn's multiple comparisons test (A: MHC-II, D, E: CD86, GAL-9), Welch ANOVA with Dunnett's T3 multiple comparisons test (E: CD155), unpaired t-test with Welch's correction (G), Mantel-Cox test for comparison of Kaplan-Meier curves. * $p < 0.05$, ** $p < 0.01$, *** $p < 0.001$, **** $p < 0.0001$.

Figure 3: Oncogene specificity influences the type of immune response to AML cells. Kaplan-Meier plot comparing survival of wildtype (WT) recipients depleted of T cells and isotype control mice when transplanted with either (A)

603 $Nras^{G12D}$ or (B) MA9 AML passaged through $Rag2^{-/-}\gamma c^{-/-}$ mice. (C) T cells from mice
604 transplanted with $Nras^{G12D}$ or MA9 AML. Histograms comparing $CD4^+$ and $CD8^+$ T
605 cell proliferation through loss of cell trace violet when cultured with or without
606 irradiated $Nras^{G12D}$ cells isolated from $Rag2^{-/-}\gamma c^{-/-}$ recipients. (D) Proliferation index of
607 $CD4^+$ or $CD8^+$ T cells (as in C) after incubation with irradiated $Nras^{G12D}$, MA9 cells or
608 untransformed BM, all isolated from $Rag2^{-/-}\gamma c^{-/-}$ recipients. Representative data from
609 replicate experiments. (E) Frequency of T cells (as a % of sytox- (alive) GFP- cells),
610 CD4+ and CD8+ T cells (as a proportion of total T cells), and CD4+ effector and
611 CD8+ effector T cells (as a % of either CD4+ or CD8+ T cells) in naïve WT mice and
612 secondary WT recipients of AML previously passaged through $Rag2^{-/-}\gamma c^{-/-}$ mice. (F)
613 Percentage of CD4+ and CD8+ T cells co-expressing PD-1, DNAM-1, KLRG1 and
614 TIM-3 from spleens of naïve C57BL/6J mice and AML recipients, n = 3-4 per
615 condition. Statistics are only displayed for double positive populations. (G)
616 Percentage of T cells expressing PDCD1 (PD-1) in the BM of healthy individuals or
617 patients with MLL-translocated or mutant RAS AML. Unpaired t-test (D: CD4+),
618 Mann-Whitney test (D: CD8+), One-way ANOVA with Tukey's p-value adjustment (E,
619 G), Welch ANOVA with Dunnett's T3 multiple comparisons test (F: PD-1+/DNAM-1+,
620 PD-1+/TIM-3+), Kruskal-Wallis test with Dunn's multiple comparisons test (F: PD-
621 1+/KLRG1+).

622 **Figure 4: $Nras^{G12D}$ AML cells escape immunologic control through**
623 **immunoediting.** (A) Experimental schema for cross-over experiment to test for
624 immunoediting. (B) Kaplan-Meier plot comparing survival of tertiary recipients
625 transplanted with 2^o $Nras^{G12D}$ passaged through either $Rag2^{-/-}\gamma c^{-/-}$ or WT mice (n = 5
626 per group). Representative data shown from two repeat experiments. (C) Kaplan-

Meier plot comparing survival of tertiary recipients transplanted with 2° MA9 passaged through either Rag2$^{-/-}$γc$^{-/-}$ or WT mice (n = 5 per group). Representative data shown from two repeat experiments. (D) Flow cytometry analysis of cell surface expression of immune modulatory molecules on N-IE and IE GFP+ Nras^{G12D} cells. MFI fold change normalized to average N-IE MFI analyzing H-2D^{b}, H-2K^{b}, MHC Class II, (E) PD-L1 and CD86. Pooled data from two experiments. (F) Experimental schema for anti-PD-1 treatment of IE Nras^{G12D} recipients. Mice were transplanted with IE Nras^{G12D} on day 0. Treatment with vehicle or anti-PD-1 (250μg per recipient) was commenced on day 7 post-transplant and continued every 3 days until day 35. (G) The proportion of tumor in a single, matched liver lobe (left), the number of tumors in a single, matched liver lobe, as quantified from H&E staining (middle) and the number of mice with tumor in a single, matched liver lobe (table) of vehicle (n=12) or anti-PD-1 (n=12) treated mice pooled from two independent experiments. Mann-Whitney test for comparison between two groups (D, E, G). * p <0.05, ** p < 0.01, *** p <0.001, **** p <0.0001.

Figure 5: Myc activation reduces immunogenicity in Nras^{G12D}-driven AML. (A) Enrichment of genes correlating with down-regulation of Nras signaling in immunoedited (IE) Nras^{G12D} AML, as determined from RNA-sequencing of GFP+ AML cells isolated from either immunocompetent WT (IE, n=5) or immunodeficient Rag2$^{-/-}$γc$^{-/-}$ (N-IE, n=5) recipients. (B) Relative quantification of Nras copy number in genomic DNA by qPCR in N-IE and IE Nras^{G12D} AML cells, expressed fold change to the N-IE mean. (C) Enrichment of genes correlating with upregulation of Myc transcriptional targets in IE Nras^{G12D} AML. (D) Correlation between the relative enrichment of a gene set containing core Myc transcriptional targets [38] and genes

associated with cytolytic infiltrate in AML [39], using bulk expression data from NRAS mutant AML patients [33]. (E) Flow cytometry analysis of cell surface expression of immune modulatory molecules on N-IE $Nras^{G12D}$ AML cells transduced with either a Myc expression construct (MYC) or empty vector (EV) and passaged in $Rag2^{-/-}\gamma c^{-/-}$ recipients (mCherry+ GFP+ CD11b+ splenocytes from 5 independent $Rag2^{-/-}\gamma c^{-/-}$ recipients). (F) Survival of $Rag2^{-/-}\gamma c^{-/-}$ and WT secondary recipients transplanted with 60,000 N-IE $Nras^{G12D}$/EV or MYC AML cells. Mantel-Cox test for comparison of Kaplan-Meier curves. Unpaired t-test (E) with Welch's correction (B). * $p < 0.05$, ** $p < 0.01$, *** $p < 0.001$, **** $p < 0.0001$.

References

1. Lane, S.W. and D.G. Gilliland, *Leukemia stem cells.* Semin Cancer Biol, 2010. **20**(2): p. 71-6.

2. Papaemmanuil, E., et al., *Genomic Classification and Prognosis in Acute Myeloid Leukemia.* New England Journal of Medicine, 2016. **374**(23): p. 2209-2221.

3. Döhner, H., D.J. Weisdorf, and C.D. Bloomfield, *Acute Myeloid Leukemia.* New England Journal of Medicine, 2015. **373**(12): p. 1136-1152.

4. Straube, J., et al., *The impact of age, NPM1(mut), and FLT3(ITD) allelic ratio in patients with acute myeloid leukemia.* Blood, 2018. **131**(10): p. 1148-1153.

5. DiNardo, C.D., et al., *Azacitidine and Venetoclax in Previously Untreated Acute Myeloid Leukemia.* N Engl J Med, 2020. **383**(7): p. 617-629.

6. Bocchia, M., et al., *Specific binding of leukemia oncogene fusion protein peptides to HLA class I molecules.* Blood, 1995. **85**(10): p. 2680-4.

7. Pollock, J.L., et al., *Murine acute promyelocytic leukemia cells can be recognized and cleared in vivo by adaptive immune mechanisms.* Haematologica, 2005. **90**(8): p. 1042-9.

8. Austin, R., M.J. Smyth, and S.W. Lane, *Harnessing the immune system in acute myeloid leukaemia.* Crit Rev Oncol Hematol, 2016. **103**: p. 62-77.

9. Lion, E., et al., *Natural killer cell immune escape in acute myeloid leukemia.* Leukemia, 2012. **26**(9): p. 2019-26.

10. Teague, R. and J. Kline, *Immune evasion in acute myeloid leukemia: current concepts and future directions.* Journal for ImmunoTherapy of Cancer, 2013. **1**(1): p. 13.

11. Toffalori, C., et al., *Immune signature drives leukemia escape and relapse after hematopoietic cell transplantation.* Nat Med, 2019. **25**(4): p. 603-611.

12. van Galen, P., et al., *Single-Cell RNA-Seq Reveals AML Hierarchies Relevant to Disease Progression and Immunity.* Cell, 2019. **176**(6): p. 1265-1281 e24.

13. Ling, V.Y., et al., *Immunological markers for prognostication in cytogenetically normal acute myeloid leukemia.* Am J Hematol, 2015. **90**(12): p. E219-20.

14. Costello, R.T., et al., *Defective expression and function of natural killer cell-triggering receptors in patients with acute myeloid leukemia.* Blood, 2002. **99**: p. 3661-3667.

15. Fauriat, C., et al., *Deficient expression of NCR in NK cells from acute myeloid leukemia: Evolution during leukemia treatment and impact of leukemia cells in NCRdull phenotype induction.* Blood, 2007. **109**: p. 323-330.

16. Sanchez-Correa, B., et al., *Human NK cells in acute myeloid leukaemia patients: analysis of NK cell-activating receptors and their ligands.* Cancer Immunol Immunother, 2011. **60**: p. 1195-1205.

17. Szczepanski, M.J., et al., *Interleukin-15 enhances natural killer cell cytotoxicity in patients with acute myeloid leukemia by upregulating the activating NK cell receptors.* Cancer Immunol Immunother, 2010. **59**: p. 73-79.

18. Behl, D., et al., *Absolute lymphocyte count recovery after induction chemotherapy predicts superior survival in acute myelogenous leukemia.* Leukemia, 2006. **20**(1): p. 29-34.

19. Muller, C.I., et al., *Hematologic and molecular spontaneous remission following sepsis in acute monoblastic leukemia with translocation (9;11): a case report and review of the literature.* Eur J Haematol, 2004. **73**(1): p. 62-6.

20. Daver, N., et al., *Efficacy, Safety, and Biomarkers of Response to Azacitidine and Nivolumab in Relapsed/Refractory Acute Myeloid Leukemia: A*

Nonrandomized, Open-Label, Phase II Study. Cancer Discov, 2019. **9**(3): p. 370-383.

21. Sallman, D., et al., *The first-in-class anti-CD47 antibody magrolimab combined with azacitidine is well-tolerated and effective in AML patients: phase 1b results.* Blood, 2020. **136**(Supplement 1): p. 330.

22. Alexandrov, L.B., et al., *Signatures of mutational processes in human cancer.* Nature, 2013. **500**(7463): p. 415-21.

23. Rajasagi, M., et al., *Systematic identification of personal tumor-specific neoantigens in chronic lymphocytic leukemia.* Blood, 2014. **124**(3): p. 453-62.

24. De Kouchkovsky, I. and M. Abdul-Hay, *Acute myeloid leukemia: a comprehensive review and 2016 update.* Blood Cancer Journal, 2016. **6**: p. e441.

25. Dohner, H., et al., *Diagnosis and management of AML in adults: 2017 ELN recommendations from an international expert panel.* Blood, 2017. **129**(4): p. 424-447.

26. Mittal, D., et al., *New insights into cancer immunoediting and its three component phases--elimination, equilibrium and escape.* Curr Opin Immunol, 2014. **27**: p. 16-25.

27. Schreiber, R.D., L.J. Old, and M.J. Smyth, *Cancer immunoediting: integrating immunity's roles in cancer suppression and promotion.* Science, 2011. **331**: p. 1565-1570.

28. Lane, S.W., et al., *Differential niche and Wnt requirements during acute myeloid leukemia progression.* Blood, 2011. **118**(10): p. 2849-56.

29. Lavau, C., et al., *Immortalization and leukemic transformation of a myelomonocytic precursor by retrovirally transduced HRX-ENL.* The EMBO Journal, 1997. **16**(14): p. 4226-4237.

30. Andrei, V.K., et al., *Transformation from committed progenitor to leukaemia stem cell initiated by MLL–AF9.* Nature, 2006. **442**(7104): p. 818.

31. Dovey, O.M., et al., *Molecular synergy underlies the co-occurrence patterns and phenotype of NPM1-mutant acute myeloid leukemia.* Blood, 2017. **130**(17): p. 1911-1922.

32. Mazurier, F., et al., *A novel immunodeficient mouse model--RAG2 x common cytokine receptor gamma chain double mutants--requiring exogenous cytokine administration for human hematopoietic stem cell engraftment.* J Interferon Cytokine Res, 1999. **19**(5): p. 533-41.

33. Verhaak, R.G., et al., *Prediction of molecular subtypes in acute myeloid leukemia based on gene expression profiling.* Haematologica, 2009. **94**(1): p. 131-4.

34. Rakhra, K., et al., *CD4+ T Cells Contribute to the Remodeling of the Microenvironment Required for Sustained Tumor Regression upon Oncogene Inactivation.* Cancer Cell, 2010. **18**(5): p. 485-498.

752 35. Kortlever, R.M., et al., *Myc Cooperates with Ras by Programming*
753 *Inflammation and Immune Suppression.* Cell, 2017. **171**(6): p. 1301-1315.e14.

754 36. Hodi, F.S., et al., *Improved survival with ipilimumab in patients with metastatic*
755 *melanoma.* N Engl J Med, 2010. **363**(8): p. 711-23.

756 37. Casey, S.C., et al., *MYC regulates the antitumor immune response through*
757 *CD47 and PD-L1.* Science, 2016. **352**(6282): p. 227-31.

758 38. Bywater, M.J., et al., *Reactivation of Myc transcription in the mouse heart*
759 *unlocks its proliferative capacity.* Nat Commun, 2020. **11**(1): p. 1827.

760 39. Dufva, O., et al., *Immunogenomic Landscape of Hematological Malignancies.*
761 Cancer Cell, 2020. **38**(3): p. 380-399 e13.

762 40. Freedman, A.S., et al., *Selective induction of B7/BB-1 on interferon-gamma*
763 *stimulated monocytes: a potential mechanism for amplification of T cell*
764 *activation through the CD28 pathway.* Cell Immunol, 1991. **137**(2): p. 429-37.

765 41. Reggiardo, R.E., et al., *Mutant KRAS regulates transposable element RNA*
766 *and innate immunity via KRAB zinc-finger genes.* Cell Rep, 2022. **40**(3): p.
767 111104.

768 42. Wellenstein, M.D. and K.E. de Visser, *Cancer-Cell-Intrinsic Mechanisms*
769 *Shaping the Tumor Immune Landscape.* Immunity, 2018. **48**(3): p. 399-416.

770 43. Matsushita, H., et al., *Cancer exome analysis reveals a T-cell-dependent*
771 *mechanism of cancer immunoediting.* Nature, 2012. **482**(7385): p. 400-4.

772 44. DuPage, M., et al., *Expression of tumour-specific antigens underlies cancer*
773 *immunoediting.* Nature, 2012. **482**: p. 405.

774 45. Takeda, K., et al., *IFN-γ is required for cytotoxic T cell-dependent cancer*
775 *genome immunoediting.* Nature Communications, 2017. **8**: p. 14607.

776 46. Shankaran, V., et al., *IFNgamma and lymphocytes prevent primary tumour*
777 *development and shape tumour immunogenicity.* Nature, 2001. **410**(6832): p.
778 1107-11.

779 47. Majzner, R.G. and C.L. Mackall, *Tumor Antigen Escape from CAR T-cell*
780 *Therapy.* Cancer Discov, 2018. **8**(10): p. 1219-1226.

781 48. Kennedy, G.A., et al., *Incidence and nature of CD20-negative relapses*
782 *following rituximab therapy in aggressive B-cell non-Hodgkin's lymphoma: a*
783 *retrospective review.* Br J Haematol, 2002. **119**(2): p. 412-6.

784 49. Christopher, M.J., et al., *Immune Escape of Relapsed AML Cells after*
785 *Allogeneic Transplantation.* N Engl J Med, 2018. **379**(24): p. 2330-2341.

786 50. Chen, D.-P., et al., *Association between single nucleotide polymorphisms*
787 *within HLA region and disease relapse for patients with hematopoietic stem*
788 *cell transplantation.* Scientific Reports, 2019. **9**(1): p. 13731.

789 51. Liao, D., et al., *A Review of Efficacy and Safety of Checkpoint Inhibitor for the*
790 *Treatment of Acute Myeloid Leukemia.* Frontiers in pharmacology, 2019. **10**:
791 p. 609-609.

52. Tran, E., et al., *T-Cell Transfer Therapy Targeting Mutant KRAS in Cancer.* The New England journal of medicine, 2016. **375**(23): p. 2255-2262.

53. Johnson, D.B., et al., *Impact of NRAS mutations for patients with advanced melanoma treated with immune therapies.* Cancer immunology research, 2015. **3**(3): p. 288-295.

54. Xu, Y., et al., *Translation control of the immune checkpoint in cancer and its therapeutic targeting.* Nature Medicine, 2019. **25**(2): p. 301-311.

55. Zimmerli, D., et al., *MYC promotes immune-suppression in triple-negative breast cancer via inhibition of interferon signaling.* Nat Commun, 2022. **13**(1): p. 6579.

56. Muthalagu, N., et al., *Repression of the Type I Interferon Pathway Underlies MYC- and KRAS-Dependent Evasion of NK and B Cells in Pancreatic Ductal Adenocarcinoma.* Cancer Discov, 2020. **10**(6): p. 872-887.

57. Lasry, A., et al., *An inflammatory state remodels the immune microenvironment and improves risk stratification in acute myeloid leukemia.* Nat Cancer, 2022.

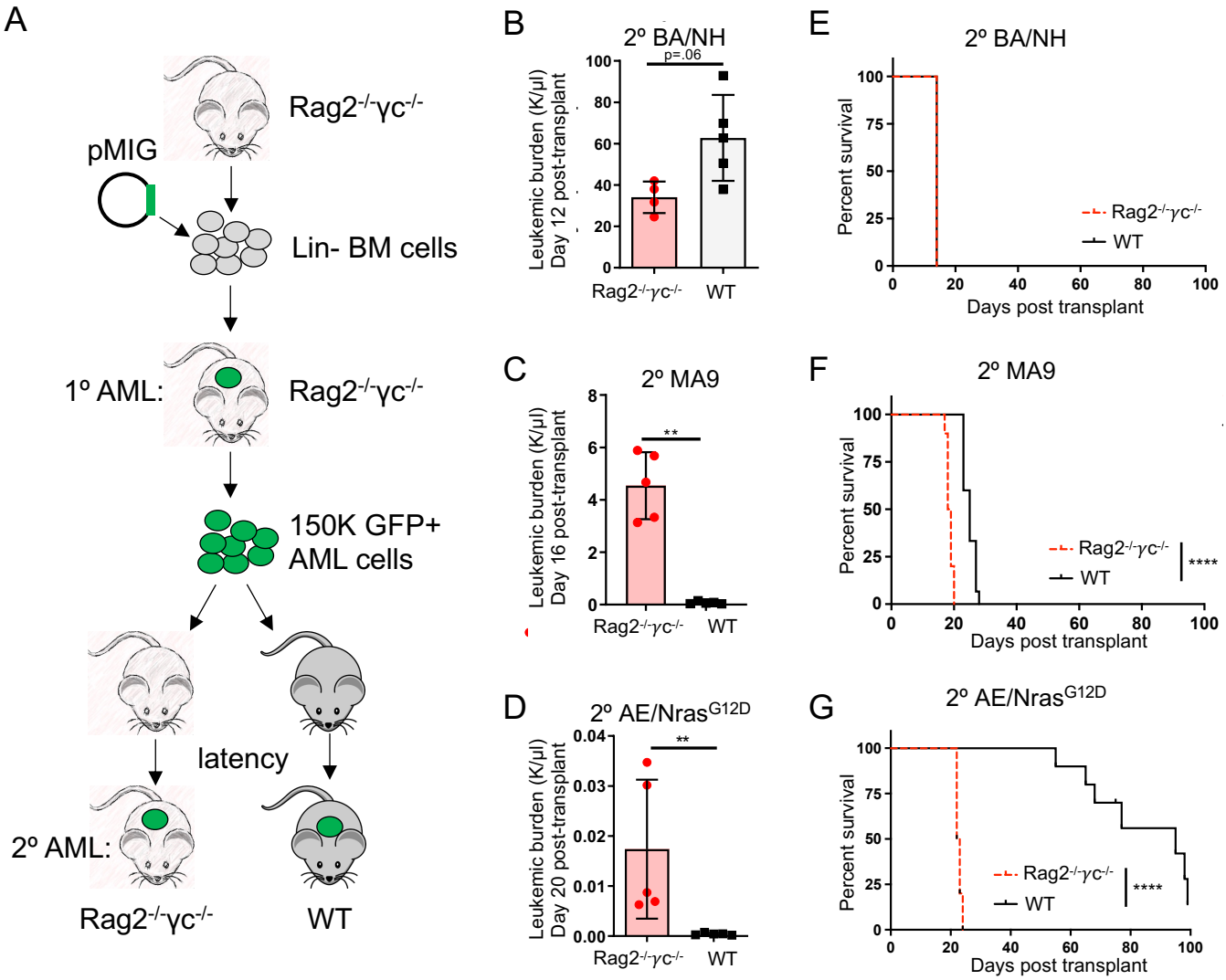
A
pMIG
Rag2-/-γc-/-
Lin- BM cells
1º AML:
Rag2-/-γc-/-
150K GFP+
AML cells
latency
2º AML:
Rag2-/-γc-/-
WT
B
2º BA/NH
p=.06
Leukemic burden (K/µl)
Day 12 post-transplant
Rag2-/-γc-/-
WT
C
2º MA9
**
Leukemic burden (K/µl)
Day 16 post-transplant
Rag2-/-γc-/-
WT
D
2º AE/NrasG12D
**
Leukemic burden (K/µl)
Day 20 post-transplant
Rag2-/-γc-/-
WT
E
2º BA/NH
Percent survival
Rag2-/-γc-/-
WT
Days post transplant
F
2º MA9
Percent survival
Rag2-/-γc-/-
WT
****
Days post transplant
G
2º AE/NrasG12D
Percent survival
Rag2-/-γc-/-
WT
****
Days post transplant

Figure 1

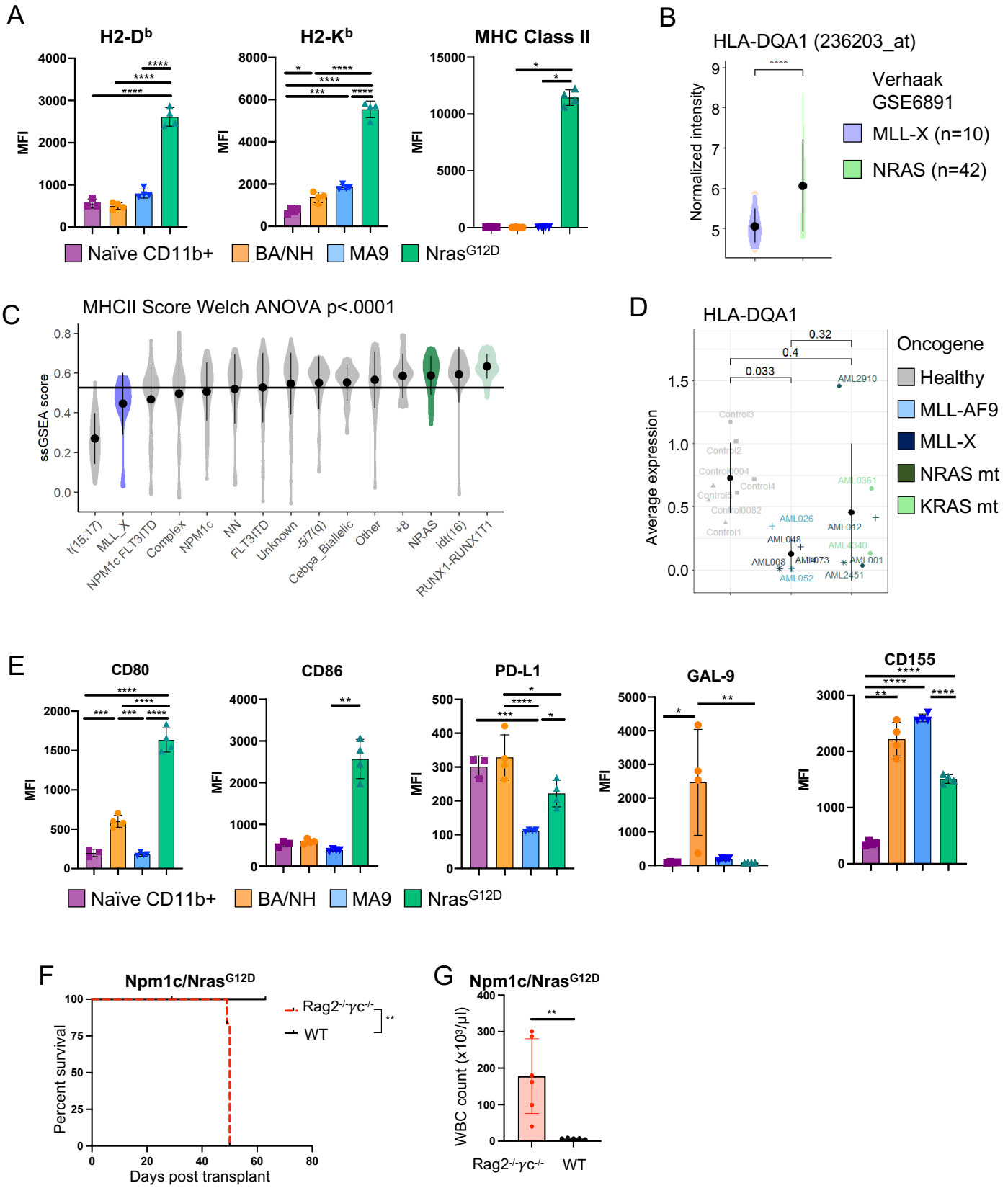
A
H2-Db
H2-Kb
MHC Class II
MFI
Naïve CD11b+
BA/NH
MA9
NrasG12D
B
HLA-DQA1 (236203_at)
Normalized intensity
Verhaak GSE6891
MLL-X (n=10)
NRAS (n=42)
C
MHCII Score Welch ANOVA p<.0001
ssGSEA score
t(15;17)
MLL_X
NPM1c FLT3ITD
Complex
NPM1c
NN
FLT3ITD
Unknown
-5/7(q)
Cebpa_Biallelic
Other
+8
NRAS
idt(16)
RUNX1-RUNX1T1
D
HLA-DQA1
Average expression
0.32
0.4
0.033
Oncogene
Healthy
MLL-AF9
MLL-X
NRAS mt
KRAS mt
AML2910
AML0361
AML026
AML012
AML048
AML340
AML008
AML073
AML001
AML052
AML2451
E
CD80
CD86
PD-L1
GAL-9
CD155
MFI
Naïve CD11b+
BA/NH
MA9
NrasG12D
F
Npm1c/NrasG12D
Rag2-/-γc-/-
WT
Percent survival
Days post transplant
G
Npm1c/NrasG12D
WBC count (x10³/µl)
Rag2-/-γc-/-
WT

Figure 2

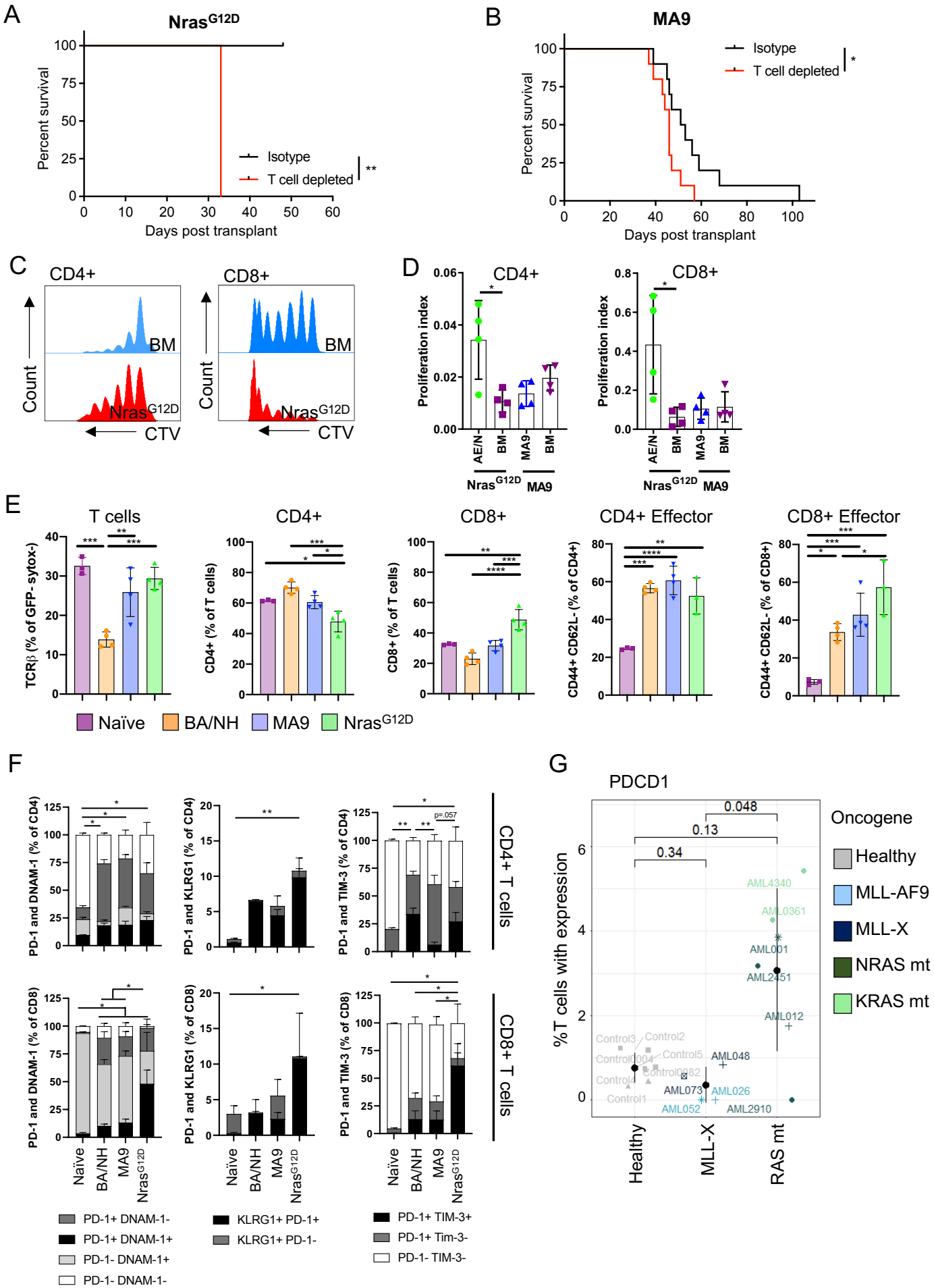
A
NrasG12D
Percent survival
Days post transplant
Isotype
T cell depleted
**
B
MA9
Percent survival
Days post transplant
Isotype
T cell depleted
*
C
CD4+
CD8+
BM
NrasG12D
Count
CTV
D
CD4+
CD8+
Proliferation index
AE/N
BM
MA9
BM
NrasG12D
MA9
E
T cells
CD4+
CD8+
CD4+ Effector
CD8+ Effector
TCRβ (% of GFP- sytox-)
CD4+ (% of T cells)
CD8+ (% of T cells)
CD44+ CD62L- (% of CD4+)
CD44+ CD62L- (% of CD8+)
Naïve
BA/NH
MA9
NrasG12D
F
PD-1 and DNAM-1 (% of CD4)
PD-1 and KLRG1 (% of CD4)
PD-1 and TIM-3 (% of CD4)
p=.057
CD4+ T cells
PD-1 and DNAM-1 (% of CD8)
PD-1 and KLRG1 (% of CD8)
PD-1 and TIM-3 (% of CD8)
CD8+ T cells
Naïve
BA/NH
MA9
NrasG12D
PD-1+ DNAM-1-
PD-1+ DNAM-1+
PD-1- DNAM-1+
PD-1- DNAM-1-
KLRG1+ PD-1+
KLRG1+ PD-1-
PD-1+ TIM-3+
PD-1+ Tim-3-
PD-1- TIM-3-
G
PDCD1
0.048
0.13
0.34
%T cells with expression
AML4340
AML0361
AML001
AML2451
AML012
Control3
Control2
Control5
Control004
Control082
Control4
Control1
AML048
AML073
AML026
AML052
AML2910
Healthy
MLL-X
RAS mt
Oncogene
Healthy
MLL-AF9
MLL-X
NRAS mt
KRAS mt

Figure 3

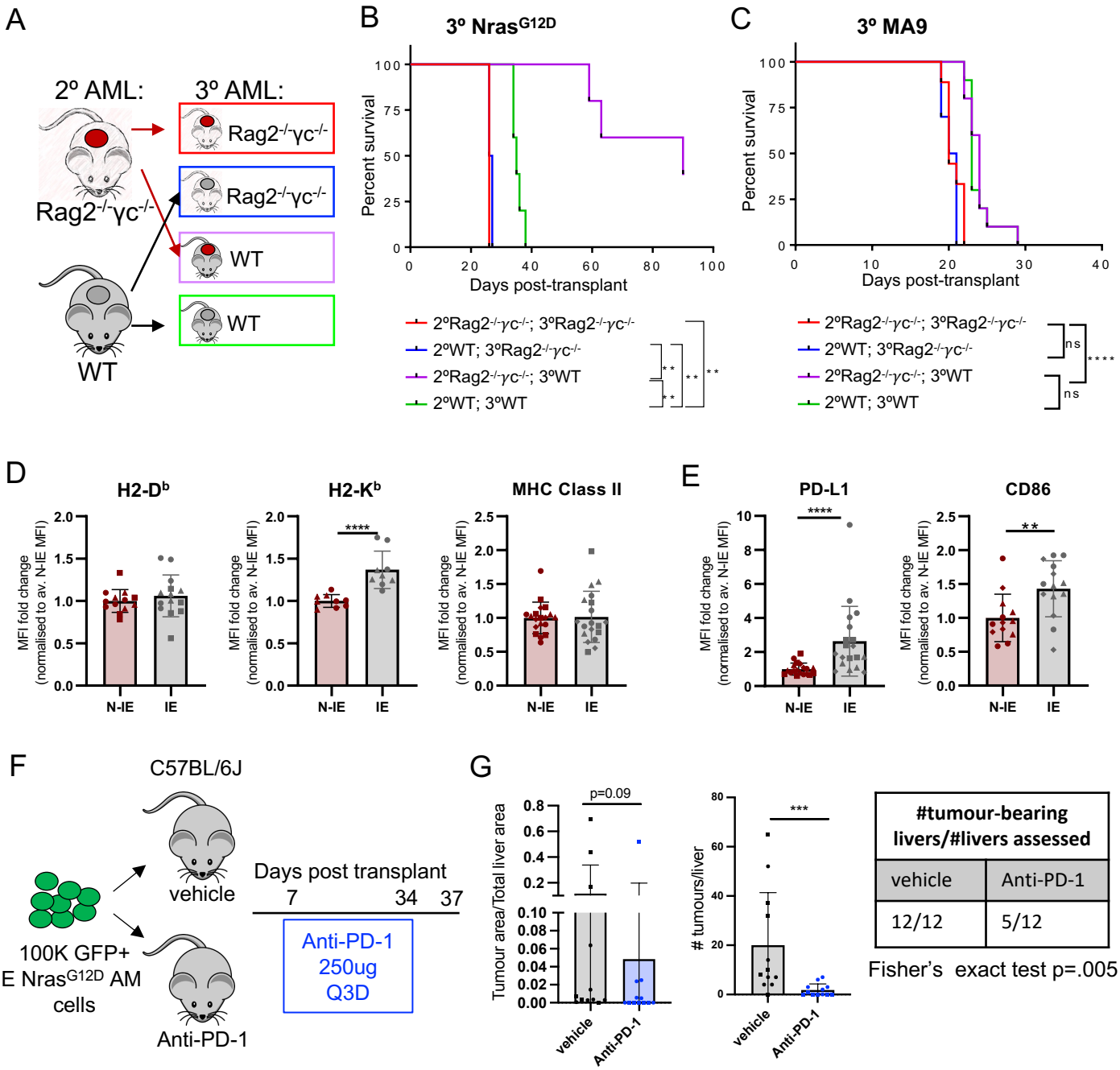

#tumour-bearing livers/#livers assessed	
vehicle	Anti-PD-1
12/12	5/12

Fisher's exact test p=.005

Figure 4

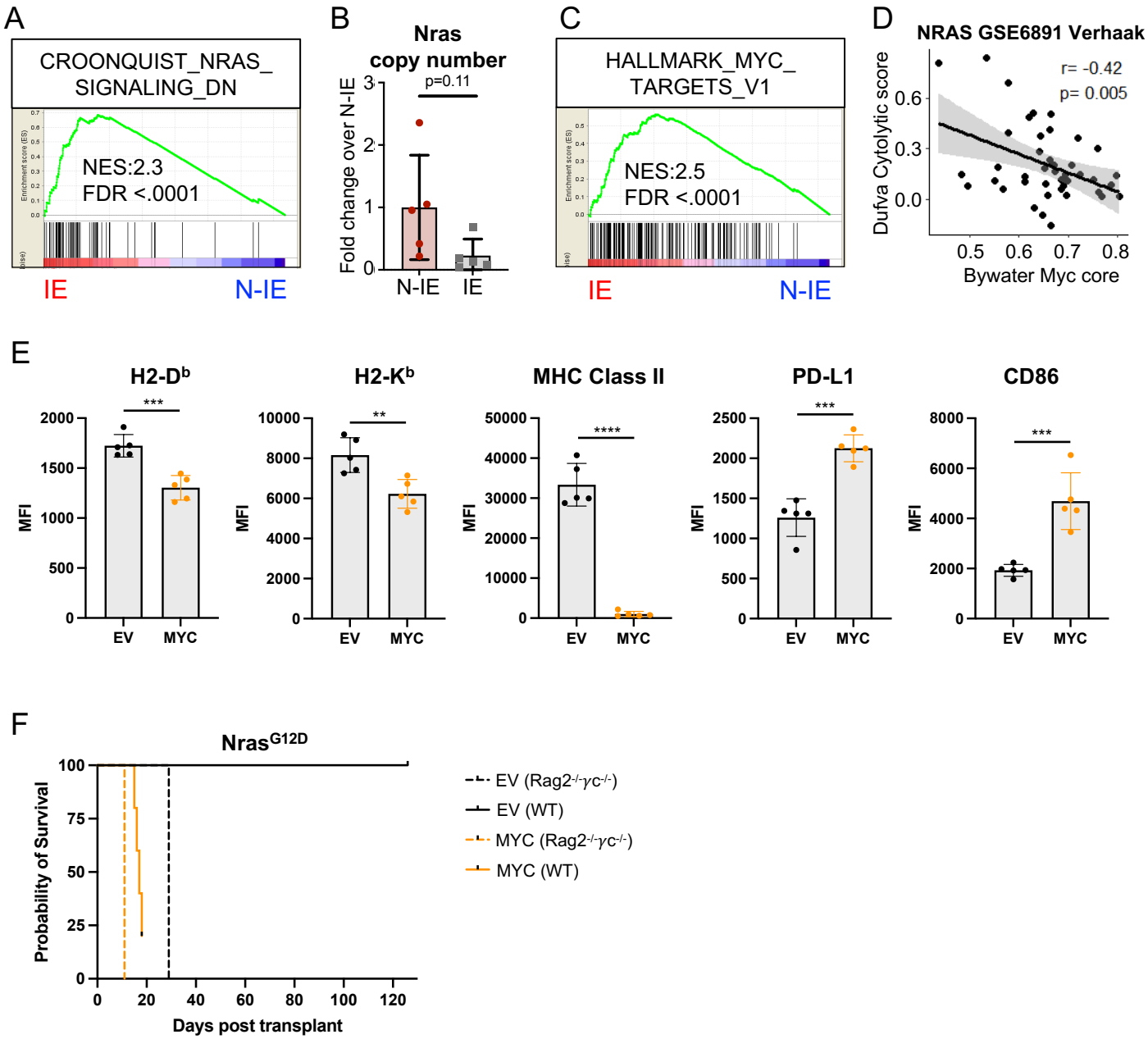
A
CROONQUIST_NRAS_
SIGNALING_DN
NES:2.3
FDR <.0001
IE
N-IE
B
Nras
copy number
p=0.11
Fold change over N-IE
N-IE
IE
C
HALLMARK_MYC_
TARGETS_V1
NES:2.5
FDR <.0001
IE
N-IE
D
NRAS GSE6891 Verhaak
r= -0.42
p= 0.005
Dufva Cytolytic score
Bywater Myc core
E
H2-Db
H2-Kb
MHC Class II
PD-L1
CD86
MFI
EV
MYC
F
NrasG12D
Probability of Survival
Days post transplant
EV (Rag2-/-γc-/-)
EV (WT)
MYC (Rag2-/-γc-/-)
MYC (WT)

Figure 5